



# ANALYSIS OF BUCKLING AND BENDING FAILURE OF ALUMINIUM COLUMN SECTIONS USED IN EMERGENCY RESTORATION TOWERS

SARAH RAMJI<sup>1</sup>, CIRO PASINI<sup>1</sup>, YONGJIAN CHANG<sup>2</sup>, and OYA MERCAN<sup>2</sup>

<sup>1</sup>*Tower Solutions Inc., Markham, Canada*

<sup>2</sup>*Dept of Civil Engineering, University of Toronto, Toronto, Canada*

This paper presents an experimental analysis of buckling and bending failure modes of a 2.58 m long, 460×460 mm<sup>2</sup> 6061-T6 Aluminum alloy column section used in emergency restoration towers. The main objective is to determine the bending and buckling load capacities of the column section through experiments, as these values are critical in an emergency tower (guyed mast) design. Within the context of this overarching goal, a secondary objective is to ascertain whether the presence of certain manufacturing non-conformance affects the loading capacity of the section significantly. Finally, finite-element analysis (FEA) simulations are conducted in order to compare the experimental data with numerical results. The results show that the ultimate bending and buckling load capacities of the column section are 383 kN and 3,868 kN respectively. Furthermore, the results indicate that the presence of manufacturing non-conformances such as air bubbles and delamination do not have a detrimental effect on the load capacity of the column. Of the two non-conformances studied, the specimen with bubbles had a 1% difference from the good specimen, and the delaminated specimen had a 10% deviation. Comparison of experimental data with FEA simulation results shows that the numerical solution tends to overestimate the stiffness of the column, and that the FEA approach may require further calibration.

*Keywords:* Modular construction, Buckling load, Bending behavior, Finite element analysis.

## 1 INTRODUCTION

High voltage transmission lines are vulnerable to breakage and service disruption when extreme weather conditions impose heavy loads on permanent towers, causing them to collapse. Emergency restoration systems (ERS) are used to temporarily restore the conductors so that electrical power can be resumed quickly, while the permanent towers are replaced. Although an extreme weather event can pass by quickly, the temporary tower must be able to withstand even extreme conditions, particularly when they are used for maintenance applications. These emergency restoration structures are essentially guyed mast structures. The tower column, or mast, consists of a 2.58 m long, 460×460 mm<sup>2</sup> 6061-T6 square aluminum section, having a corner rail that permits the travel of a safety tether and a hoisting apparatus, allowing line workers to remain attached at all times. These masts can be joined together to form a column of any desired height, held in place by guy wires. These masts are essential to the strength of the emergency tower, and determination of the number and position of guy wires required for the tower design, and hence accurate determination of the properties of these emergency tower sections is

beneficial. The main objective of this paper is to analyze the bending and buckling failure of an aluminum section used in emergency restoration towers through experiments. A secondary objective of the present study is to determine whether the presence of manufacturing non-conformances such as bubbles and delamination has a detrimental effect on the loading performance of the column section. Finally, a comparison between FEA results and experimental data is made for both bending and buckling to gain a better understanding of the validity of the numerical simulations.

## 2 LITERATURE REVIEW

Some previous studies have presented testing results for aluminum alloy hollow section columns. Zhu and Young (2006) investigated the behavior of circular hollow aluminum column sections. They studied the effects of welding on aluminum alloy columns and observed that the experimental ultimate load of welded columns was 54-76 % of the ultimate load corresponding to the non-welded columns. They also developed a non-linear finite element model and found that the numerical models developed matched the experimental results. Zhu and Young (2008) also conducted compression and bending tests for circular, square and rectangular section aluminum beam columns. Fan *et al.* (2013) tested a series of aluminum alloy H-type sections fabricated using 6082-T6 heat-treated aluminum alloy subject to axial compression between two pinned ends. The overall buckling and axial load bearing capacities were obtained. Dimopoulos and Gantes (2012) investigated the experimental and numerical behavior of cantilevered shells with opening and stiffening, which reflected the geometric characteristics of wind turbine tunnels.

## 3 EXPERIMENTAL SETUP, RESULTS, AND DISCUSSION

### 3.1 Test Procedure and Setup

The bending and buckling tests on the tower section (mast, or column) were conducted using the Baldwin Universal Testing Machine at the Department of Civil Engineering, University of Toronto. This is a large-scale test machine capable of applying both tension and compression loads up to 5400 kN, on specimens up to 6 m high. For both these tests, the loads were applied using a pin connection at the top – a 610 mm diameter plate that can rotate to a maximum of 4 degrees. The load cases, maximum load applied before failure and the nature of the specimens tested are listed in Table 1.

For the buckling test shown in Figure 1, the load is applied on the top along the vertical axis of the tower modular section specimen via a pivoting head connection. A 600×600×50 mm<sup>3</sup> steel plate is fixed to the bottom of the modular tower section by 8 ASTM A324 bolts in order to fix the end of the column on the ground. The bending test was conducted by setting the specimen on two roller supports 100 mm distance away from the ends, as shown in Figure 2. The bending load is applied at the middle of the modular section via a pivoting head connection and a steel plate.

Table 1. Load case, specimen type, and maximum load for all tests.

No.	Load Case	Specimen type	Max load (kN)
1	Bending1	Rejected specimen (with bubbles)	383.88
2	Bending2	Good specimen	386.08
3	Buckling1	Rejected specimen (with bubbles)	3868.4
4	Buckling2	Good specimen	3801.5
5	Buckling3	Good specimen	3822.6
6	Buckling4	Good specimen	3735.4
7	Buckling5	Delaminated specimen	3351.6

Local strain and stress were determined using strain gauges. These gauges were positioned at areas predetermined to be critical from an initial FEA simulation. Based on the results of these tests, the number of strain gauges was adjusted for the subsequent tests. The gauges were also subsequently concentrated on areas where failure was determined to occur from the initial experimental tests, particularly on the heat affected zones (HAZ) of the aluminum welds. Figure 3 and 4 show the location of strain gauges for the bending and buckling tests, respectively.

The load for the buckling tests was increased at a rate of approximately 1.75 kN/s before the yield point, and 0.65 kN/s after. For the bending test, the load was initially increased at a rate of approximately 0.4-0.6 kN/s, and the load rate was dropped to approximately 0.2 kN/s once the welds cracked. The load-displacement relationship, load-local strain relationship, and the failure modes of all the specimens were captured during the experiments. In addition, the maximum load carrying capacity, the ultimate compressive displacement, and the initial stiffness of the tower modular section specimens were determined.



Figure 1. Buckling test experimental setup.



Figure 2. Bending test experimental setup.

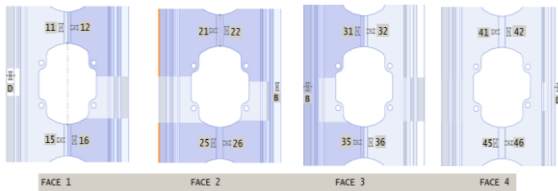


Figure 3. Strain gauge locations for bending tests.



Figure 4. Strain gauge locations for buckling tests.

### 3.2 Bending Tests

Two bending tests were conducted, and the results were compared with the FEA simulations. The maximum loads reached before failure for first (rejected) and second (good specimen) experimental tests before failure were 383 kN and 386 kN, respectively, as shown in Figure 5. In the corresponding FEA simulation, the maximum load reached before failure was almost two times greater than the experimental values, and the initial stiffness was marginally higher in the

FEA. Comparisons between the experimental results of the two specimens showed that the maximum displacements for the rejected specimen were 23.5 mm and for the good specimen was 28.5 mm. Comparing failure modes, the reject specimen had six ‘drop’ points, each of which indicates cracking in the aluminum welds. As the load increased over the load bearing capacity of the welds, they cracked, causing the applied load to decrease. This is evidenced by the drop in the load-displacement curves. For the test of the ‘good’ specimen, only two of the welds fail, implying that the aluminum section had carried a greater load beyond the ultimate tensile strength of the material. Figure 6 shows the two specimens at the completion of the tests, and Table 2 provides the stress values as determined by the strain gauges. It is observed that the values are mostly below the yield stress of 275 MPa.

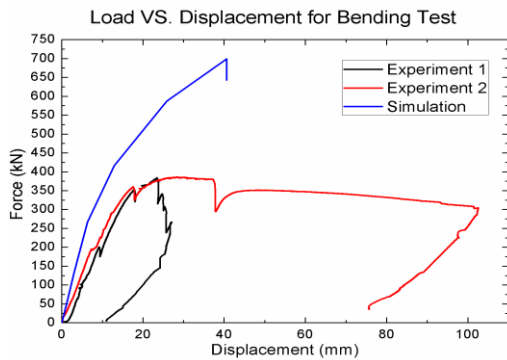


Figure 5. Load-displacement curves for the bending tests.

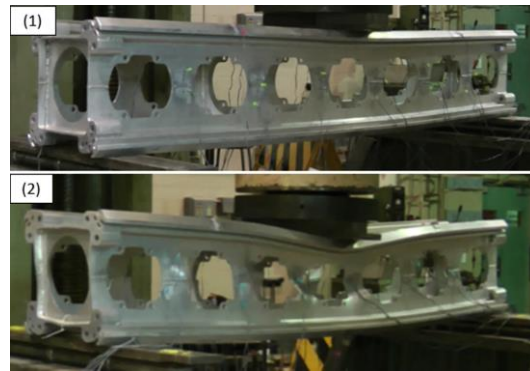


Figure 6. The specimens at the completion of bending test 1 and 2.

Table 2. Results of the bending tests.

	Corner D Stress (MPa)	Face 1 Stress (MPa)				Face 2 Stress (MPa)				Corner B Stress (MPa)
Location		11	12	15	16	21	22	25	26	
Simulation	203.4	13.4	92.8	197.7	4.1	-145.3	-18.9	-23.3	-121.4	204.0
Bending 1		-42.2	167.6	-32.7	200.1	<b>-284.5</b>	43.0	60.2	168.7	130.4
Bending 2		289.9	-111.0	<b>281.9</b>	-141.2	-88.4	<b>-558.0</b>	152.9	157.9	139.5
	Corner B Stress (MPa)	Face 3 Stress (MPa)				Face 4 Stress (MPa)				Corner D Stress (MPa)
Location		31	32	35	36	41	42	45	46	
Simulation	204.0	5.3	-30.6	-4.9	3.3	-127.5	-62.8	-20.8	-158.0	203.4
Bending 1	130.4	-8.6	29.8	-7.6	41.3	149.9	-77.1	-275.8	42.5	
Bending 2	139.5	165.4	-41.6	193.2	-44.8	272.1	204.6	-72.1	-558.0	

### 3.3 Buckling Tests

As mentioned earlier, five specimens were used for the buckling tests, and the loads applied before failures are listed in Table 1. The load-displacement curves for these five specimens are shown in Figure 7. The displacements ranged from 30 mm to 38 mm, and the initial stiffness for

each test is almost the same. The FEA simulation shown in Figure 8 indicated a higher initial stiffness, but the same maximum load, as shown in Figure 7. As mentioned before, the first two buckling tests used the maximum number of strain gauges, which were strategically positioned near the welds between each hole. Figure 4 shows the initial location of the strain gauges, and Table 3 shows the corresponding stress values. Stress values obtained for locations 11, 12, 21, and 22 are omitted from the table since the measured stress is not critical at those locations. It can be seen that most values measured by the strain gauges are in the elastic range, and only a few are beyond the yield strength. It is further observed that the strain gauges showing readings in the plastic range are predominantly in the corners of the specimen.

The first two tests showed that the critical portions of the section are around the third hole of the tower section, where global buckling was observed. Strain gauges were thus increased at this location. Table 3 shows the results of these tests, which are similar to the first two buckling tests. However, it can be observed that the strain gauges concentrated around the third hole of the tower section have reached their saturation point, which corresponds to a stress of 558 MPa. Finally, considering the two manufacturing non-conformances studied, the specimen with bubbles did not have any observed strength reduction, while the delaminated specimen failed at a load approximately 10% lower than the other specimens.

Table 3. Results of the buckling tests at the locations and corners shown for each of the 6 simulations

	D (MPa)	Face 1 Stress (MPa)				A (MPa)	Face 2 Stress (MPa)				B (MPa)
Location		13	14	15	16		23	24	25	26	
Simulation	-244.4	-315.9	-298.0	-22.9	-2.9	-253.0	-296.7	-293.9	2.5	-14.6	-176.4
Buckling 1	/	/	/	87.9	<b>281.6</b>	<b>-351.1</b>	/	/	180.5	-100.1	/
Buckling 2	<b>-558.0</b>	/	/	176.7	130.8	/	/	/	95.8	<b>-284.6</b>	268.6
Buckling 3	-240.0	<b>-558.0</b>	<b>-558.0</b>	22.0	12.6	-198.3	<b>-558.0</b>	<b>-558.0</b>	36.9	31.6	-179.9
Buckling 4	278.4	<b>-558.0</b>	<b>-558.0</b>	95.1	<b>-558.0</b>	<b>-558.0</b>	<b>-558.0</b>	<b>-558.0</b>	103.3	39.6	-345.7
Buckling 5	-82.2	<b>-558.0</b>	<b>-558.0</b>	/	/	281.1	-327.6	<b>-558.0</b>	/	/	217.0
	B (MPa)	Face 3 Stress (MPa)				C (MPa)	Face 4 Stress (MPa)				D (MPa)
Location		33	34	35	36		43	44	45	46	
Simulation	-176.4	-298.1	-303.3	-13.2	12.2	-180.5	-317.6	-314.2	12.7	-15.7	-244.4
Buckling 1	/	/	/	<b>-277.6</b>	77.1	-266.2	/	/	48.5	-74.5	/
Buckling 2	268.6	/	/	-72.1	48.3	/	/	/	-53.8	98.9	<b>-558.0</b>
Buckling 3	-179.9	<b>-558.0</b>	<b>-558.0</b>	-28.3	57.1	-182.1	<b>-558.0</b>	<b>-558.0</b>	33.5	-49.6	-240.0
Buckling 4	-345.7	<b>-558.0</b>	<b>-558.0</b>	143.0	202.0	287.9	<b>-558.0</b>	<b>-558.0</b>	-63.9	9.4	278.4
Buckling 5	217.0	<b>-558.0</b>	<b>-558.0</b>	-295.3	67.5	<b>-558.0</b>	<b>-558.0</b>	<b>-558.0</b>	/	/	-82.2

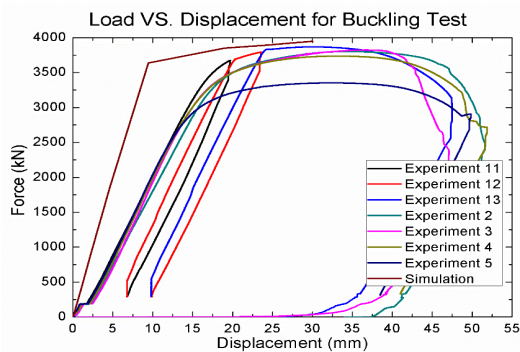


Figure 7. Load-displacement curves for the buckling tests.

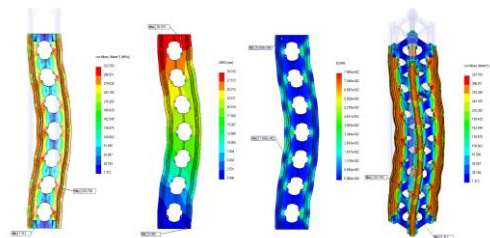


Figure 8. FEA simulation results for the buckling test.

### 3.4 Stress-Strain Curve

Using load-displacement curves discussed above and the local strain measurements from the strain gauges obtained during the experiment, the strain values can be translated into stresses given the stress-strain relationship of the aluminum alloy. The elastic modulus is 69,000 MPa; the yield strength is 275 MPa, and the ultimate tensile strength is 310 MPa. A simplified stress-strain relationship was also obtained from an FEA analysis and is shown in Figure 9. The local stresses are obtained from this curve.

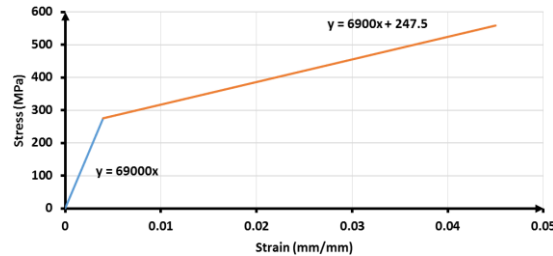


Figure 9. Simplified stress-strain curve for the aluminum alloy.

## 4 CONCLUSIONS

This paper investigates the bending and buckling load capacity of an aluminum column section used in Emergency Restoration Towers. The maximum bending and buckling load capacities of the column section are 383 kN and 3,868 kN, respectively. Moreover, the presence of certain manufacturing non-conformances does not reduce the maximum load capacity of the section significantly. The bubble non-conformances reduce the bending load capacity by less than 1% without reducing the buckling capacity. The delaminated specimen shows an approximately 10% reduction in buckling capacity. Finally, a comparison of experimental results with FEA simulations shows that the numerical stiffness tends to be underestimated by the FEA approach, and that the FEA approach requires further calibration.

### Acknowledgments

The authors acknowledge financial support from the Government of Canada's NSERC ENGAGE program and thank Harry Sildva and Lino Borroto for their early contributions.

### References

- Dimopoulos, C. A., and Gantes, C. J., Experimental Investigation of Buckling of Wind Turbine Tower Cylindrical Shells with Opening and Stiffening Under Bending, *Thin-Walled Structures*, 54, 140-155, March 2012.
- Fan, F., Wang, Y., Lin, L., and Qian, H., Experimental Study on Axial Compression Performance of High-Strength Aluminum-Alloy Columns with H-Section, *Applied Mechanics and Materials*, 274, 459-462, 2013, January 2013.
- Zhu, J. H., and Young, B., Experimental Investigation of Aluminum Alloy Circular Hollow Section Columns, *Engineering Structures*, 28, 207-215, January 2006.
- Zhu, J. H., and Young, B., Numerical Investigation and Design of Aluminum Alloy Circular Hollow Section Columns, *Thin-Walled Structures*, 46, 1437-1449, December 2008.